

CHAPTER 31

Orthonormal Wavelet Analysis for Deep-Water Breaking Waves

Nobuhito MORI * and Takashi YASUDA †

ABSTRACT

This study aims to develop a method using wavelet transform to detect wave breaking event from temporal water surface elevation data. Sudden surface jump associated with breaking wave is regarded as shock wave and shock wavelet spectrum is defined to detect the occurrence of the surface jump. The visual observation of breaking wave crest shows that this method can almost completely detect the occurrence of breaking wave in random wave trains.

1. INTRODUCTION

Wave breaking plays important roles in numerous aspects of horizontal and vertical momentum transfer from surface waves to current and mixing of surface layer. Since breaking waves are associated with steep and giant waves, wave breaking is very important phenomenon to estimate their upper limit and the occurrence probability of their wave height. Furthermore, breaking waves exert the strong wave induced force, which occasionally bring about impact pressure to structures.

A great deal of effort has been made on direct observations of wave breaking in the ocean. One of them is direct visual observation of white caps to detect the breaking waves [Holthuijsen & Herbers(1986)], because the wave breaking is related to some sort of instability near the crests. Since they required much efforts, the visual observations are not adequate to ordinary routine observation. Another approach is to detect the breaking events in the time series of surface elevation, directly. Longuet-Higgins & Smith(1983) observed breaking waves by using a surface jump meter. Recently, Su & Cartmill(1993) developed a

*Graduate student, Graduate School of Gifu University, Yanagido, Gifu 501-11, Japan.

†Professor, Dept. of Civil Eng., Gifu University, Yanagido, Gifu 501-11, Japan.

new detection method of breaking wave by a void fraction technique. These direct measurement methods are quite well but require special and sophisticated instrument, so that they are not also in general use. Weissman *et al.*(1984) measured energy backscattering of the high frequency components due to wave breaking with the running Fourier spectrum method. Their detection method is empirical and has not objectivity, nevertheless their method need not any special instruments. They use the Fourier spectrum analysis that is generally effective to analyze an energy change, periodicity and a power law of data. However, it is not suitable to use unsteady process such as breaking. The reason why the Fourier analysis has not temporally or spatially local information on data is that its integral basis consists of periodic function.

Recently, a new method of aperiodic and unsteady data analysis which has a locally confined integral basis, so-called '*wavelet analysis*', is getting well known[for example, Meyer(1991) and Farge(1992)]. Shen *et al.*(1994) studied local energy characteristics of wind generated waves using a continuous wavelet transform. Since the continuous wavelets, however, have overcomplete basis which causes formal relations among expansion coefficients, they are not suitable to analyze local energy properties. Meyer(1989) studied and formulated the orthogonal analyzing wavelet system. This orthogonal wavelet transform is known as adequate analysis of the local energy characteristics of the data[Mori *et al.*(1993)].

In this study we make a rational breaking wave detection scheme to indicate and to measure small jumps and discontinuities in surface elevation associated with breaking waves. Further, we check the validity of the method by experimental data and analyze the local energy properties of breaking wave using the orthonormal wavelet analysis.

2. PRINCIPLE OF MEASUREMENT

2.1 Orthonormal wavelet expansion

Since the kernel functions of continuous wavelet transforms are not mutually orthogonal, we have the redundancy of wavelet coefficients independent of data. The excellent mathematical formulation of orthogonal analyzing wavelet, *multi-resolution analysis*, was developed by Mallat(1989). Accordingly, in this paper, we employ the orthonormal wavelet expansion to analyze a water surface elevation.

The orthogonal wavelet expansion of an arbitrary function $\eta(t)$ is written as

$$\eta(t) = \sum_{j=1}^{\infty} \sum_{k=1}^{\infty} \alpha_{j,k} \psi_{j,k}(t), \quad (j, k \in Z) \quad (1)$$

in which $\alpha_{j,k}$ ($j, k \in Z$, where Z is the set of all integers) is an expansion coefficient and $\psi_{j,k}(t) \in L(\mathbf{R}^2)$ is a complete orthonormal set of wavelets generated from an analyzing wavelet, which is sometimes called mother wavelet, by discrete translations k and is corresponding to temporal position of time $k/2^j$, and discrete dilations j corresponds to frequency. It is conventional to take the discrete dilation as

$$\psi_{j,k}(t) = 2^{\frac{j}{2}} \psi(2^j t - k), \quad (j, k \in Z) \quad (2)$$

with the orthonormality condition. From the orthogonality, the wavelets allow us to obtain the expansion coefficient $\alpha_{j,k}$ in Eq.(1) by taking the innerproduct of $\eta(t)$ and $\psi_{j,k}^*(t)$ as

$$\alpha_{j,k} = \int_{-\infty}^{\infty} \eta(t) \psi_{j,k}^*(t) dt. \quad (3)$$

There are typically three types of the orthonormal analyzing wavelets as Meyer's, Daubechies' and Battle-Lemariés's. To investigate the complete relation to the Fourier analysis for the purpose of this study, we follow Meyer's method(1989) which has the properties that; i) $\psi(t)$ is a real analytic function, ii) $\psi(t)$ and its derivatives of any order are rapidly decreasing functions, iii) the moments of any order are zero, and iv) the Fourier transform of $\psi(t)$ has a compact supported in the Fourier space.

We define the mother function $\tilde{\phi}(\omega)$ of analyzing wavelet that is an infinitely differentiable real function satisfying the following conditions,

$$a) \left. \begin{aligned} \tilde{\phi}(\omega) &\geq 0, \\ \tilde{\phi}(\omega) &= \tilde{\phi}(-\omega), \\ \tilde{\phi}(\omega) &\text{ is monotonically decreasing for } \omega \geq 0, \end{aligned} \right\} \quad (4)$$

$$b) \left. \begin{aligned} \tilde{\phi}(\omega) &= 1 \quad (|\omega| \leq 2\pi/3), \\ &= 0 \quad (|\omega| \geq 4\pi/3), \end{aligned} \right\} \quad (5)$$

$$c) \{ \tilde{\phi}(\omega) \}^2 + \{ \tilde{\phi}(\omega - 2\pi) \}^2 = 1 \quad (2\pi/3 \leq |\omega| \leq 4\pi/3). \quad (6)$$

The conditions of a) to c) do not uniquely determine $\tilde{\phi}(\omega)$, so that we can make arbitrary functions $\tilde{\phi}(\omega)$, if $\tilde{\phi}(\omega)$ satisfies the above conditions of a) to c). We employ here the mother function $\tilde{\phi}(\omega)$ defined as

$$\tilde{\phi}(\omega) = \sqrt{g(\omega)g(-\omega)}, \quad (7)$$

where

$$g(\omega) = \frac{h(4\pi/3 - \omega)}{h(\omega - 2\pi/3) + h(4\pi/3 - \omega)}, \quad (8)$$

$$h(\omega) = \begin{cases} \exp(-1/\omega^2), & (\omega > 0) \\ 0, & (\omega \leq 0) \end{cases} \quad (9)$$

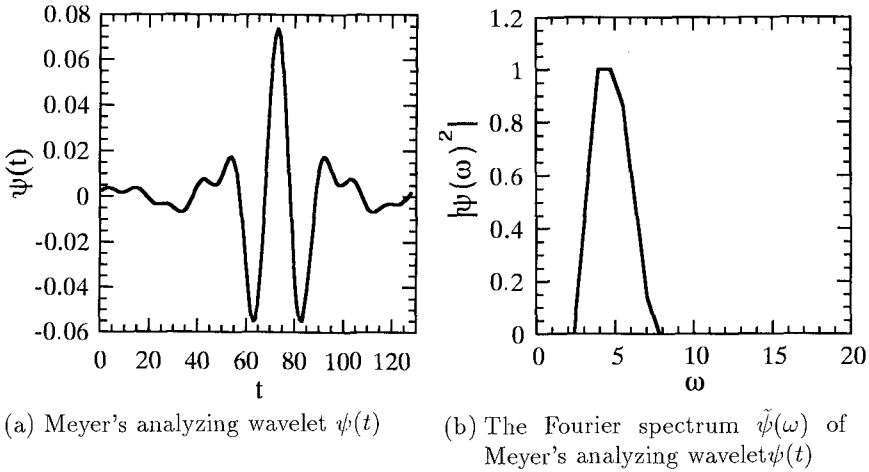


Figure 1: Illustrations of Meyer's analyzing wavelet.

which is the same definition of Yamada & Ohkitani(1990).

From the conditions of a) to c) and Eqs.(7) to (9), the Fourier coefficients of analyzing wavelet $\tilde{\psi}(\omega)$ are defined as

$$\tilde{\psi}(\omega) = e^{(-i\omega/2)} \sqrt{\{\tilde{\phi}(\omega/2)\}^2 - \{\tilde{\phi}(\omega)\}^2}. \tag{10}$$

Note that $\tilde{\phi}(\omega)$ has a compact support in $\{\omega \mid 2\pi/3 \leq |\omega| \leq \pi/3\}$. Therefore, the wavelet coefficient is directly connected to the Fourier coefficient.

The inverse Fourier transform of $\tilde{\psi}(\omega)$ gives the following desired analyzing wavelet,

$$\psi(t) = \frac{1}{2\pi} \int_{-\infty}^{\infty} \tilde{\psi}(\omega) e^{i\omega t} d\omega. \tag{11}$$

Fig.1 shows Meyer's analyzing wavelet and its Fourier spectrum. The analyzing wavelet is very regular. However, it is not very well localized in physical space but is supported compact in the Fourier space. The fast algorithm for wavelet transform with Meyer's analyzing wavelet using FFT algorithm is formulated by Yamada & Ohkitani(1991).

2.2 Relation between the wavelet and the Fourier spectra

It could be worth pointing out that the relations between the wavelets and the Fourier spectra. Meyer's analyzing wavelet has a useful property that is the compactness of the support in the Fourier space. Eq.(6) shows that $\tilde{\psi}(\omega)$ is only included in $[-2^{j+3}\pi/3, -2^{j+1}\pi/3] \cup [2^{j+1}\pi/3, 2^{j+3}\pi/3]$. Since the square of wavelet coefficient is corresponding to the energy, the direct relation between

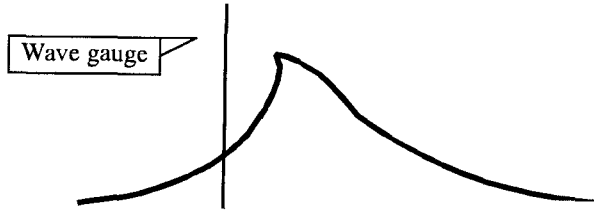


Figure 2: Illustration of breaking wave passing a wave gauge.

the wavelet and the Fourier spectrum is expected as

$$E_j = \sum_{k=1}^{\infty} |\alpha_{j,k}|^2 \sim \omega S(\omega) \quad (\omega \sim 2^{j+2} \pi/3) \quad (12)$$

where ω is angular frequency, $S(\omega)$ the Fourier spectrum and E_j the wavelet spectrum. Particularly, the relationship of a power law of the energy spectrum between the wavelet and the Fourier spectrum can be expressed as

$$E_j \sim 2^{-j(p-1)} \iff S(\omega) \sim \omega^{-p}. \quad (13)$$

Eq.(13) gives the relation that ω^{-p} in the Fourier spectrum is equivalent to $2^{-j(p-1)}$ in the wavelet spectrum.

2.3 Local and shock wavelet spectra

The purpose of this study is to detect jumps in water surface elevation associated with breaking. We suppose that the sea surface elevation $\eta(t)$ is measured as a function of time t with a discrete sampling time Δt at a fixed horizontal position as illustrated in Fig.2. The wave passing the sensor will generally show a smooth rise $\partial\eta/\partial t$. But, if a just breaking wave passes the sensor, we can expect a sudden jump of the surface elevation. The magnitude of the sudden jump is associated with the scale of breaker type: *i.e.* for a plunging breaker this is relatively large and it is smaller for spilling breaker.

The Fourier series of shock wave represented as

$$y(t) = \begin{cases} At, & t \leq 0.5, \\ A(t-1), & t \geq 0.5, \end{cases} \quad (0 \leq t \leq 1) \quad (14)$$

where A is the height of shock is easily given by $\sum(-4/n) \sin(n\omega t)$. Therefore, a power law of the energy spectrum of the breaking wave with the sudden jump is expected to ω^{-2} or 2^{-j} .

To investigate the local energy information among the scale, we define the local wavelet spectrum $L_{j,k'}$ for the scale $j \geq j_s$ as

$$L_{j,k'} = \sum_{k'} |\alpha_{j,k}|^2, \quad (0 \leq k' \leq 2^{j_s}) \quad (15)$$

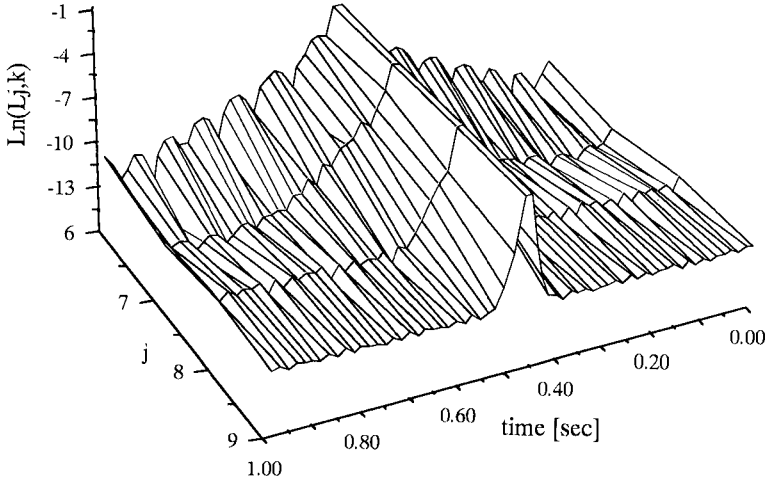


Figure 3: The local wavelet spectrum $L_{j,k'}$ of shock wave given by Eq.(14).

where, j_s is minimum dilation mode of the local wavelet spectrum which determine the resolution and \sum denotes the special summation over k satisfying: $(k/2^{j_s} \leq k'/2^j \leq (k + 1)/2^{j_s})$. The local wavelet spectrum $L_{j,k'}$ can analyze characteristics of microscopic or local energy properties for data. Besides, we introduce the shock wavelet spectrum to detect the surface jump of the shock wave described by Eq.(14). The shock wavelet spectrum $M_{j,k'}$ is defined by following as

$$M_{j,k'} = 2^j \times \sum_{k'} |\alpha_{j,k}|^2. \quad (0 \leq k' \leq 2^{j_s}) \tag{16}$$

Since power law of shock wave is 2^{-j} for the wavelet spectrum, that is corresponding to power law of ω^{-2} for the Fourier spectrum, the shock wavelet spectrum detects the shock as a constant power whenever jumps observed in the surface elevation.

Fig.3 shows the local wavelet spectrum($j_s=6$) for the shock wave given by Eq.(14). The number of points to discretize the shock wave is 512. The local wavelet spectrum shows the energy distribution of *time-frequency* space and indicates existence of the high crest corresponding the time of shock at $t=0.5$. This result implies the effectiveness of the local wavelet spectrum for local energy analysis. To make clear the local energy properties of the shock wave, the shock wavelet spectrum($j_s=6$) for shock wave of Eq.(14) is shown in Fig.4. We can easily detect the shock from the characteristic structures of shock wavelet spectrum $M_{j,k'}$ both of the occurrence time and their magnitudes.

To say nothing of the accuracy of detection of shock depend on discretization of data. The relation sampling frequency Δt and the local power law is shown

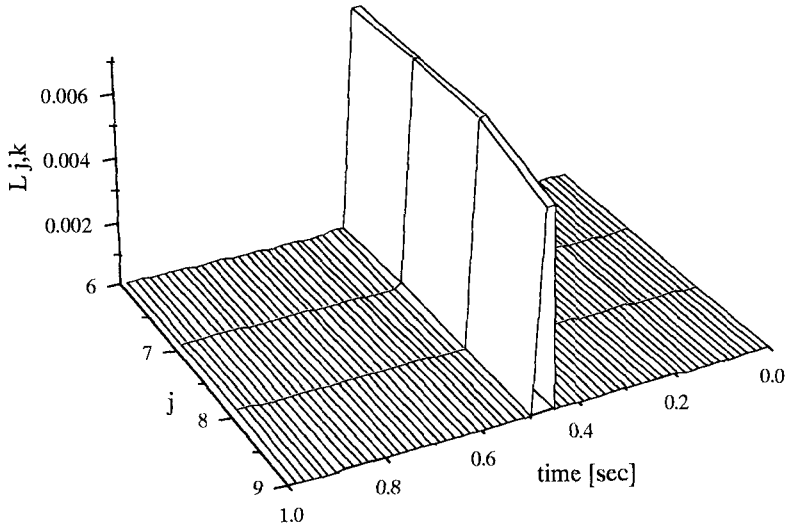


Figure 4: The shock wavelet spectrum $M_{j,k'}$ of shock wave given by Eq.(14).

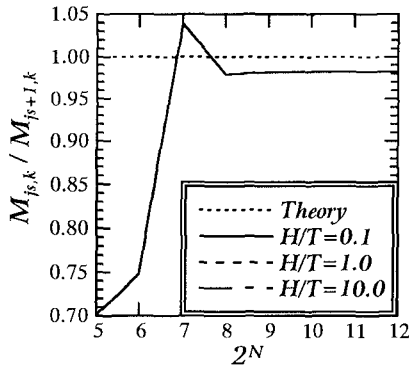


Figure 5: Comparison of the local power law of shock wave between the numerical and analytical one.

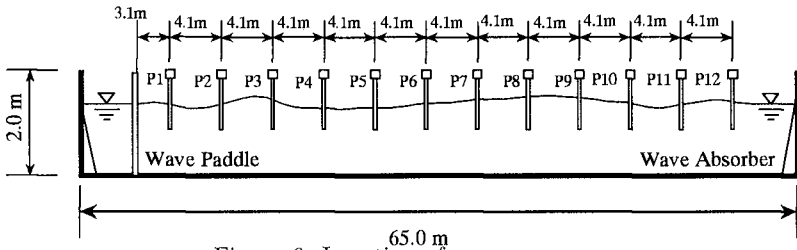


Figure 6: Location of wave gages.

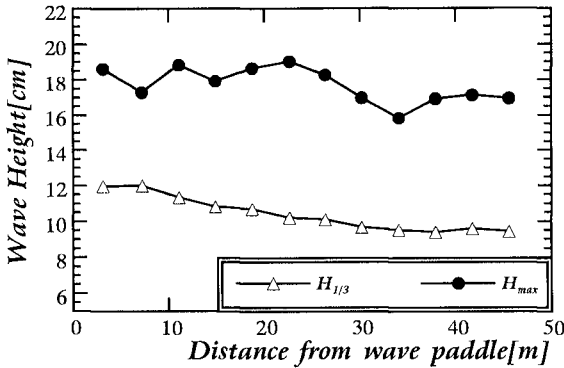


Figure 7: Spatial variation of the wave height statistics.

in Fig.5, where H is the height of the shock wave and T is the wave period. The value of j_s is set equal to $j_{max}-2$ and the local power law of the wavelet spectra are calculating the scales between the j_s and $j_s + 1$. The error of estimating of power law is 2.7% for $N=256$ to 4096, 4% for $N=128$, 25% for $N=64$ and 30% for $N=32$. We conclude that the number of point $N \geq 64$ or 128 per one wave is required to accurate estimation the jump from the data. Note that the accuracy of estimation is independent of the amplitude of the shock wave.

3. EXPERIMENTS

3.1 Experimental condition

The experiments were conducted in the glass channel installed at Technical Research & Development Institute of Nishimatsu construction Co.,Ltd. The channel is 65m long, 1m wide, 2m high and was filled to a depth of 0.98m. Waves were generated by computer-controlled piston type wave paddle. The initial spectra of the surface elevations are composed of the Wallop type spectra with the band width $m=10$ and the peak frequency $f_p=1\text{Hz}$, giving a wavenumber $k_p=4.072\text{m}^{-1}$ and characteristic water depth $k_p h=3.99$, so that the waves

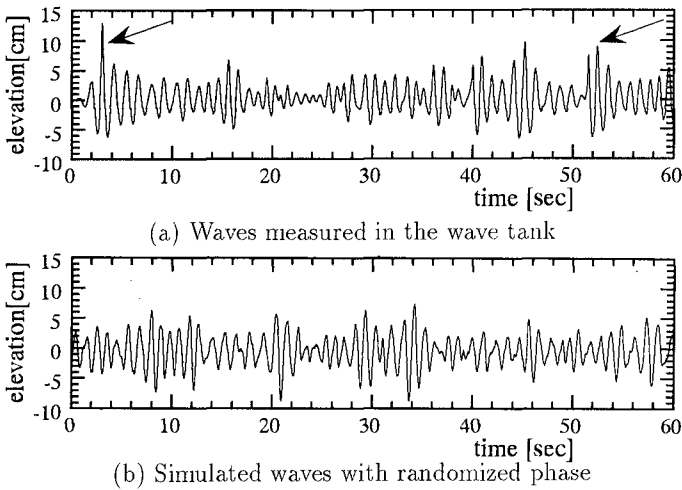


Figure 8: Water surface elevations of the random wave trains.

were deep water waves. Water surface displacements were measured with twelve capacitance type wave gages as shown in Fig.6. The measurements were performed at a sampling frequency of 100Hz for over 100sec. At the same, spatial surface profiles were recorded by video camera to examine the breaking event.

Figure 7 shows the spatial variation of H_{max} and $H_{1/3}$. Although, the value of H_{max} is fluctuated, the spatial variation of $H_{1/3}$ shows that there is some energy dissipation due to the wave breaking. In the following, we only focus the surface elevations at P5.

3.2 Local energy characteristics of nonlinear wave

The values of skewness and kurtosis at P5 are 0.245 and 3.473, so that the waves are found to have weakly nonlinear characteristics. For comparison with the experimental data, we calculate artificial random phase wave data(linear waves) which is obtained by the inverse Fourier transform of the original surface elevations of P5 after randomizing their phases uniformly over $[0, 2\pi]$ with their amplitudes unchanged. The surface elevations of experimental data and simulated wave with randomized wave are shown in Fig.8, respectively. The two arrows in the Figure indicate the time when breaking event just occurs.

Weissman *et al.*(1984) developed the detection method of breaking waves based on the singularities of the high frequencies, which is the intrinsic frequency of gravity-capillary waves, by a trial and error method with the running Fourier transform. The wave profile band-passed of high frequencies(10-12Hz) shown in Fig.8(a) is illustrated in Fig.9. The bursts of energy in the high frequency com-

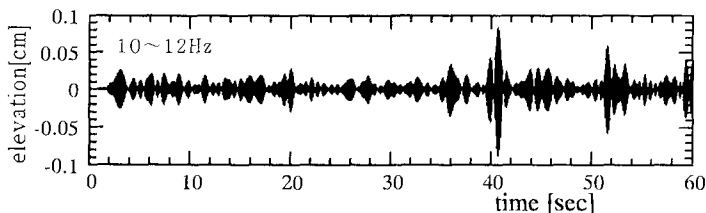


Figure 9: Water surface profile of band-pass filtered wave with the high frequency components(10-12Hz) of Fig.8(a).

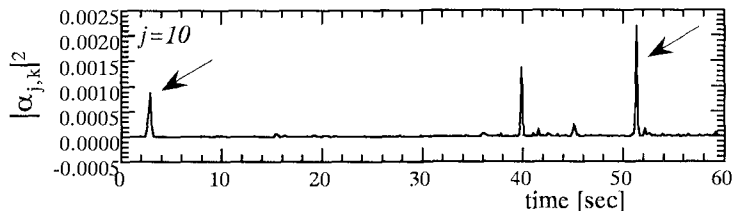
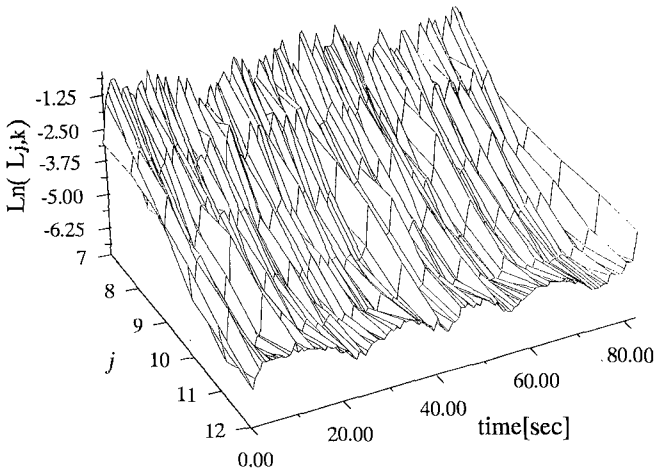


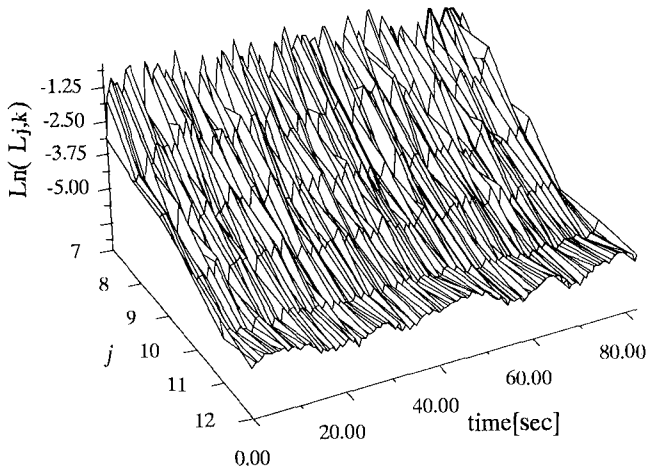
Figure 10: Temporal distribution of the square value of wavelet coefficient, $|\alpha_{j,k}|^2$, of the experimental wave

ponents are indicative of breaking events. He detected wave breaking from burst of the temporal energy distributions in this frequency band. Fig.10 shows the square value of wavelet coefficients $\alpha_{j,k}$ at the scale $j=10$ which is corresponding to about 8Hz. The distributions of square values of $\alpha_{j,k}$ clearly indicate the singularities of the high frequencies, which are corresponding to the time of breaking waves, in comparison with the result of the Fourier band filtered method(Fig.9). The same empirical method to detect the breaking waves can be applied by the wavelet analysis and will be given better result rather than the running Fourier transform, but let us then considered here the energy structure and energy cascade process among lower and higher frequency components.

It was already shown that the local wavelet spectrum is effective to analyze the temporal energy structures in previous section. Fig.11 shows the local wavelet spectra with $j_s=7$ for the experimental wave and the simulated wave, respectively. The experimental data indicate that characteristic structure of energy distribution is shown running in parallel with the j -axis. Particularly, some big crests can be observed at the large scale into small scale. Although the Fourier spectrum is the same as experimental wave, there is no pattern or structure in the local wavelet spectrum as the experimental wave in the simulated wave(b) and they seem to distributing uniformly. This implies that the high frequency components of experimental wave, nonlinear wave, are not constant in amplitude and that there are sharp peaks sporadically distributed along the time series. In other words, the high frequency components are intermittent in



(a) Waves measured in the wave tank



(b) Simulated waves with randomized phase

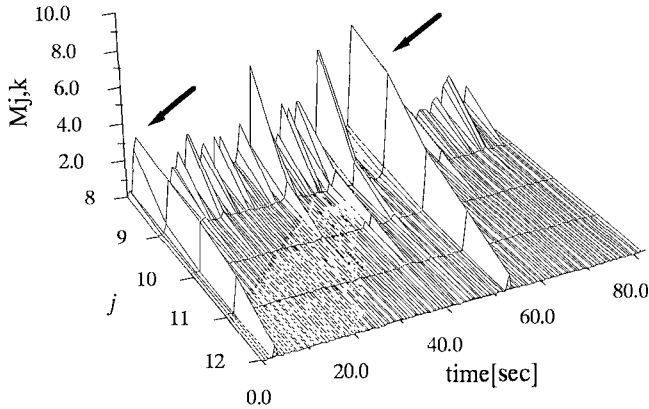
Figure 11: Local wavelet spectra for the measured and simulated waves.

the nonlinear wave.

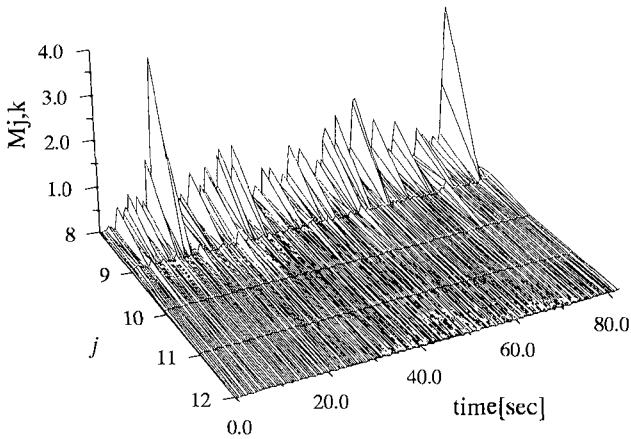
The sharp peaks and structures in wavelet space(j, k) are related with nonlinear wave-wave interaction but we leave the details to further studies.

3.3 Detection of breaking wave

The nonlinear waves have the local energy characteristics as already shown in Fig.11. This will lead us further into a consideration of detection of breaking



(a) Waves measured in the wave tank



(b) Simulated waves with randomized phase

Figure 12: Shock wavelet spectra for the measured and simulated wave.

wave by shock wavelet spectra. The shock wavelet spectra of experimental wave and simulated wave are shown in Fig.12. The sharp peaks are shown intermittently in the experimental wave, corresponding to the time when breaking wave passes. Therefore, we need some detector function to judge whether they break or not. Thus, we define the detector function a_i is calculated as

$$a_i = \frac{M_{j_s+m,k_i}}{M_{j_s,k_i}}, \tag{17}$$

where subscript i denotes temporal position ($0 \leq k^i \leq 2^{j_s}$), j_s is resolution of scale parameters and m is distance between the j_s . The illustration of the

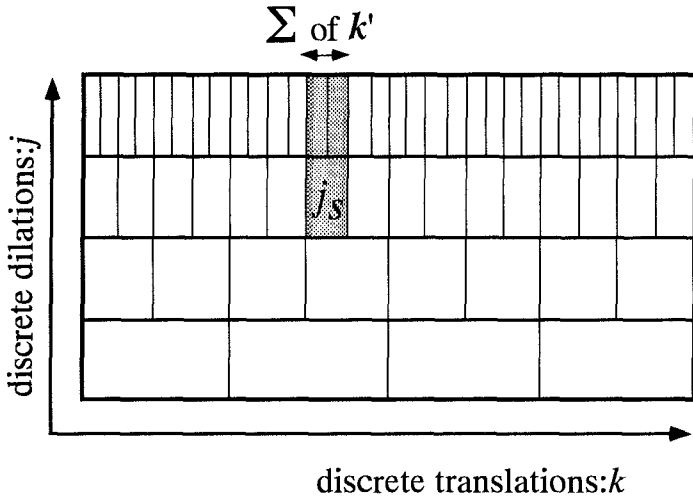


Figure 13: Illustration of wavelet space and relationship with parameters

Table 1: Accuracy of the present detection method

$a \setminus n$		$j_s=7$	$j_s=7$	$j_s=8$	$j_s=8$
		$m=1$	$m=2$	$m=1$	$m=2$
0.9	(-1)	2	1	3	2
0.8		3	1	4	2
0.6		4	1	5	2
0.5	(-2)	5	1	5	3

wavelet space and the relationship with parameter is shown in Fig.13. The experimental result of detection of the method for the experimental wave is shown Table 1 ($j_s=7$ is corresponding peak frequency of the spectrum). The actual number of breaking waves is two, therefore, $j_s=8$, $m=2$, $a_i=0.9$ and 0.8, 0.6 and $j_s=7$, $m=1$, $a_i=0.9$ gives quite nice value when we selected. The fine resolution scale of $j_s=8$ accurately detect the breaking waves rather than $j_s=7$ and the $m=2$ gives more accurate results than $m=1$. The reason for this result is sampling frequency of shock and fluctuation of the local power law due to the external noise of data.

It could be concluded that the present method can detect the breaking wave from the temporal water surface elevation data, if the adequate parameters a and m are selected as $a_i \geq 0.8$ and $m=2$.

4. CONCLUSION

We applied the orthonormal wavelet expansion to the water surface elevations of random waves and studied their local characteristics. It is found that the sudden surface jumps associated with the breaking waves were well reflected in the shock wavelet spectra. Thus, we developed the rational detection method of breaking wave as following procedure:

- 1.The wavelet coefficients $\alpha_{j,k}$ of the surface elevations are calculated Eq.(3).
- 2.The appropriate resolution with the scale j_s is selected.
- 3.The shock wavelet spectra are calculated with Eq.(16).
- 4.The local power law of the surface elevations are calculated Eq.(17).
- 5.Breaking waves are expected to have the local power a law 2^{-j} of the wavelet spectrum

Furthermore, the sudden surface jumps can be well detected, if they are described by using sufficiently many discretized points. We demonstrated the validity of the method by comparing with the experimental data. Note that this method can be applied to not only deep water waves but also shallow water.

ACKNOWLEDGEMENT

The authors are grateful to Dr.Yamada at University of Tokyo for valuable advice and wish to thank Technical Research & Development Institute of Nishimatsu construction Co.,Ltd. for their cooperation. One of the authors is supported by fellowships of the Japan Society for the Promotion of Science for Japanese Junior Scientists. Further, this research is supported in part by Grant-in-Aid for Scientific Research(JSPS-0440), The Ministry of Education, Science and Culture.

REFERENCES

- Farge, M. (1992) Wavelet transforms and their applications to turbulence, *Annual.Review.Fluid Mech.*, 24, pp.395-457.
- Holthuijsen, L.H. & T.H.C.Herbbers(1986) Statistics of breaking waves observed as whitecaps in the open sea, *J.Phys.Oceanogr*, 16, pp.290-297.
- Kennedy, R.M. & Snyder, R.L.(1983) On the formation of whitecaps by threshold mechanism Part II: Monte Carlo experiments, *J.Phys.Oceanogr*, 13, pp.1493-1504.
- Longuet-Higgins, M.S. & N.D.Smith(1983) Measurement of breaking waves by a surface jump meter, *J.Geo.Res.*, 88, C14, pp.9823-9831.

- Mallat, S.(1989) Multiresolution approximations and wavelet orthonormal bases of $L^2(R)$, *Tans.Am.Math.Soc.*, 315, pp.69-89.
- Meyer, Y.(1989) Wavelets, eds. J.M. Combes *et al.*, (Springer).
- Meyer, Y.(1991) Wavelets and Applications, (Masson-Springer).
- Mori, N., T.Yasuda & M.Yamada(1993) Orthonormal wavelet expansion and its application to water waves, *Proc.40th Coastal Eng.Conf., JSCE*, 40-1, pp.141-145(in Japanese).
- Shen, Z., W.Wang & K.Mei(1994) Finestructure of wind waves analyzed with wavelet transform, *J.Phys.Oceanogr.*, 24, pp.1085-1094.
- Su, M.Y. & J.Cartmill(1993) Breaking wave measurement by a void fraction technique, *WAVE'93*, pp.951-962.
- Weissman, M.A., S.S.Ataktürk and K.B.Katsaros(1984) Detection of breaking events in a wind-generated wave field, *J.Phys.Oceanogr*, 14, pp.1608-1619.
- Yamada, M. & K.Ohkitani(1990) Orthonormal wavelet expansion and its application to turbulence, *Prog.Theor.Phys.*, 83, No.5, pp.819-823.
- Yamada, M. & K. Ohkitani(1991) An identification of energy in turbulence by orthonormal wavelet analysis, *Prog.of Theoretical Phys.*, 86, No.4, pp.799-815.